Journal of Catalysis 344 (2016) 236–241

Contents lists available at ScienceDirect

Journal of Catalysis

journal homepage: www.elsevier.com/locate/jcat

Engineering surface structure of petroleum-coke-derived carbon dots to enhance electron transfer for photooxidation

Xiaodong Shao [†], Wenting Wu [*,†], Ruiqin Wang, Jinqiang Zhang, Zhongtao Li, Yang Wang, Jingtang Zheng, Wei Xia, Mingbo Wu [*]

State Key Laboratory of Heavy Oil Processing, China University of Petroleum, Qingdao 266580, China

ARTICLE INFO

Article history:
Received 10 July 2016
Revised 5 September 2016
Accepted 7 September 2016

Keywords:
Carbon dot
Petroleum coke
Surface structure
Electron transfer
Photooxidation

ABSTRACT

Many abundant and inexpensive materials are being developed for the synthesis of carbon dots. However, the structures of most raw materials are complicated, which inevitably bring difficulties for the optimization of their photocatalytic ability, especially for the electron transfer properties. Herein, petroleum coke was selected as raw material to prepare carbon dots (CDs). The types and contents of the functional groups —C=O and/or —S=O) on CDs surface were finely tuned by facile chemical oxidation, enhancing both of the electron-accepting (11.9 and 3.5 times) and electron-donating abilities (1.7 and 1.4 times). The photocatalytic efficiency of the optimized carbon dots (C-120) in the photooxidation of 1,4-dihydro-2,6-dimethylpyridine-3,5-dicarboxylate (1,4-DHP) is 6.6 times higher than that of CDs with few functionalized groups. The present study demonstrates a feasible and effective strategy to solve the poor electron transfer difficulty of CDs and also helps to understand the regulating strategies and mechanisms of surface structure.

© 2016 Elsevier Inc. All rights reserved.

1. Introduction

Since their discovery in 2004, [1] carbon dots (CDs) have become a research hotspot due to their superior properties, such as high aqueous solubility [2,3], outstanding biocompatibility [4–6], broadband absorbing ability [7,8], and others [9,10]. To achieve scalable and cost-effective preparation, many abundant and inexpensive materials have been developed for the synthesis of CDs. For example, Tour et al. [11] reported a facile approach to synthesizing tunable graphene quantum dots from coal. Furthermore, Qiu [12] tailored inexpensive coal to fluorescent CDs via a combined method of carbonization and acidic oxidation etching. Petroleum coke, a byproduct in the oil refining process, has been demonstrated to be good raw material for production of porous carbons [13]. Petroleum coke is rich in benzene rings or aromatic domains and contains a graphene structure that makes it possible to prepare high-performance CQDs. In addition, most of these studies focused on the photoluminescent properties of CDs [14]. Actually, CDs themselves show great potential for photocatalysis, and there is much room left for improvement of the functionalized CDs derived from inexpensive and abundant raw materials for photocatalysis.

Photocatalysis involves three key steps: absorption of photons, electron–hole separation and transfer, and subsequent surface redox reactions [15,16]. Among these steps, electron transfer plays a key role in photooxidation reactions, which has been studied extensively [3,17]. Kang [18] prepared CDs/C_3N_4 composites to improve the efficiency of electron transfer due to the fabrication of heterojunctions. For CDs themselves, the Cu–N dopant was used to enhance the efficiency of electron transfer [3]. However, these strategies are hardly employed with CDs derived from raw materials. Actually, many functional groups, such as —C=O and —S=O, are strong electron-withdrawing groups and can easily be introduced onto the surfaces of CDs by chemical methods. To some extent, they could influence the band structure and the impetus of electron transfer, which has rarely been reported.

Here, petroleum coke, a byproduct in oil refining processes, was selected as the raw material for preparing CDs due to its abundant benzene rings or aromatic domains and graphene structure [14,13]. The surface structures of CDs were tuned by chemical oxidation with a mixture of concentrated H_2SO_4 and HNO_3 (C-120, C-180) or only with HNO_3 (H-120, H-180) at different temperatures (120 and 180 °C), where H_2SO_4 was used to tune —S=O and the temperature was used to alter the content of —C=O. The surface structures of CDs were confirmed by transmission electron microscopy (TEM), X-ray diffraction (XRD), Raman, FT-IR and XPS. After the introduction of —C=O, the electron-accepting ability of C-120

* Corresponding authors.
E-mail addresses: wuwt@upc.edu.cn (W. Wu), wumb@upc.edu.cn (M. Wu).
† These authors contributed equally to this work.

http://dx.doi.org/10.1016/j.jcat.2016.09.006
0021-9517/© 2016 Elsevier Inc. All rights reserved.

is 11.9 times higher than that of C-180, while the electron-accepting property of C-120 is 3.5 times higher than that of H-120, as a result of the introduction of —S═O. At the same time, the electron-donating ability of C-120 is 1.7 and 1.4 times higher than those of C-180 and H-120, respectively. It is believed that the presence of —C═O and —S═O can influence the electron transfer process, giving rise to distinct photocatalytic performance.

2. Experimental

2.1. Synthesis of carbon dots

Materials synthesis: Petroleum coke (2.0 g) was added into a mixture of concentrated H_2SO_4 (45.0 mL, 18 M) and HNO_3 (15.0 mL, 15.2 M) or into HNO_3 (60 mL, 15.2 M) alone in a flask under ultrasonic conditions for 2 h, and then refluxed under constant stirring in an oil bath at 120 or 180 °C for 12 h, respectively. After the reaction, the mixture was cooled to room temperature and diluted 10 times with deionized water and neutralized with ammonia to pH 7.0. The neutralized mixture was filtered by a filter membrane (0.22 μm) to remove the larger fractions, yielding a solution containing CDs that was further dialyzed with MD 34 (3500 Da) for 72 h to remove the remaining salts and tiny fragments.

Reduction of CDs: Portions of 1 g phenylhydrazine (99%, Aldrich) and 1 mL HCl acid (38%) were dissolved in 200 mL $CHCl_3$, and then 500 mg CDs was added into the solution. After stirring under N_2 for 72 h, the precipitate was filtered out and washed with $CHCl_3$ in Soxhlet extractor for 20 h to remove the physical adsorbed molecules, such as phenylhydrazine. The precipitate was dried under vacuum at 60 °C for 24 h to make R-120.

2.2. Sample characterization

Transmission electron micrograph (TEM) images were taken on a JEOL JEM-2100UHR microscope with an accelerating voltage of 200 kV. X-ray powder diffraction (XRD) was performed using a PANalytical X-ray diffractometer equipped with Cu*K*α radiation (λ = 0.15406 nm, 40 kV, 40 mA). Further evidence for the composition of the product was inferred from X-ray photoelectron spectroscopy (XPS) using an ESCALAB 250Xi spectrometer equipped with a prereduction chamber. Fourier transform infrared (FT-IR) spectra were recorded on a Nicolet 6700 spectrometer. Raman spectroscopy was performed using an Ar^+ ion laser at 514.5 nm (Renishaw in Via 2000 Raman microscope, Renishawplc, UK) to assess the graphitic structure of raw materials and products. UV–vis absorption spectra were measured by a DRSUV-2450 UV–vis spectrophotometer (Shimadzu, Japan). Fluorescence spectra were measured by an F-97 Pro spectrofluorometer (Shanghai Lengguang Technology Co., Ltd., China).

2.3. Photooxidation of 1,4-DHP

Photooxidation was carried out according to a modified method from the literature [19]. An ethanol/water mixed solvent (1:1 v/v, 20 mL) containing 1,4-DHP (1.0×10^{-4} M) and the photosensitizer (CDs) were put into a two-necked round-bottom flask (50 mL). The solution was then irradiated using a xenon lamp with a power of about 35 W (600 W m^{-2}, λ = 385–800 nm) through a cutoff filter (0.72 M $NaNO_2$ solution, which is transmittal for light with λ > 385 nm). UV–vis absorption spectra were recorded at intervals of 2–5 min. The consumption of 1,4-DHP was monitored by the decrease in absorption at 374 nm, and the concentration of 1,4-DHP was calculated using its molar absorption coefficient (ε = 7744 M^{-1} cm^{-1}).

2.4. Electron spin resonance spectroscopy

Electron spin resonance (ESR) spectra were recorded at room temperature using a JEO JES FA200 spectrometer at 9.8 GHz, X-band, with 100 Hz field modulation. Samples were quantitatively injected into specially made quartz capillaries for ESR analysis in the dark and illuminated directly in the cavity of the ESR spectrometer. All optical measurements were performed at room temperature.

3. Results and discussion

3.1. Modifying the surface structure of carbon dots

Since the functionalized groups (e.g., —C═O and —S═O) show strong electron-withdrawing ability, they have a great potential to tailor the photooxidation properties of materials. Here, CDs were carefully prepared by chemical oxidation of petroleum coke with a mixture of concentrated sulfuric acid and nitric acid under different temperatures, (120 and 180 °C, namely C-120 and C-180, respectively. The various temperatures provide a facile way to tune the —C═O content of CDs. When the temperature is lower than 120 °C, CDs are difficult to obtain. As the temperature exceeds 180 °C, the functionalized groups (—C═O) easily escape as gaseous byproducts from the solution, causing a decrease in oxygen-containing functional groups on the surface of CDs [20]. At the same time, H_2SO_4 was used to introduce —S═O. For comparison, H-120 and H-180 with no —S═O (in contrast to C-120) were prepared with only HNO_3 at 120 and 180 °C, respectively. To some extent, the number of these functionalized groups on CDs could be finely controlled by the preparation temperature and chemical oxidant. Furthermore, the sizes of CDs were uniformly confined by the dialysis for the sake of eliminating the size-confinement effects. Here, C-120 with rich oxygen-containing functional groups was selected as a good candidate for photooxidation, which is proved in Section 3.3.

3.2. Characterization of the petroleum-coke-derived carbon dots

The morphology and physical structure of CDs were studied by TEM, XRD, and Raman spectroscopy. Fig. S1a in the Supplementary Material shows the particle size distribution of C-120, revealing that the diameter of C-120 is about 1.7 nm. The insets in Fig. S1a are typical high-resolution TEM (HRTEM) images of C-120, which indicates a certain crystallinity with a lattice space of 0.33 nm, corresponding to the lattice fringes of the (002) planes of graphite [21]. The XRD and Raman spectroscopic results are consistent with these results (Figs. S1b and S1c) [22,23], supporting the formation of a graphite-like structure, which is assumed to be beneficial for electron transfer during the photocatalysis.

The functional groups on the surface of C-120 were studied by FT-IR and XPS spectra (Fig. 1b–d). Obviously, they are packed with oxygen functional groups. The small peaks at 1608 cm^{-1} are caused by a carbonyl group (C═O) conjugated with the benzene ring stretching vibration. The existence of sulfonic groups is demonstrated by the characteristic absorption bands at 1065 and 651 cm^{-1}, which are assigned to the symmetric stretching of S═O and the C—S stretching vibration, respectively. As the reaction temperature increases, the content of C═O decreases sharply (Fig. 1b and c). When the temperature reaches 180 °C, there is little C═O in C-180, which could be attributed to the deep oxidation of C═O into carbon dioxide [20]. These results are consistent with those of XPS (Fig. 1b). The XPS spectrum of C1*s* (Fig. 1c) from CDs can be deconvoluted into three smaller peaks, which are ascribed to the following functional groups: sp^3 bonded carbon (C—C,

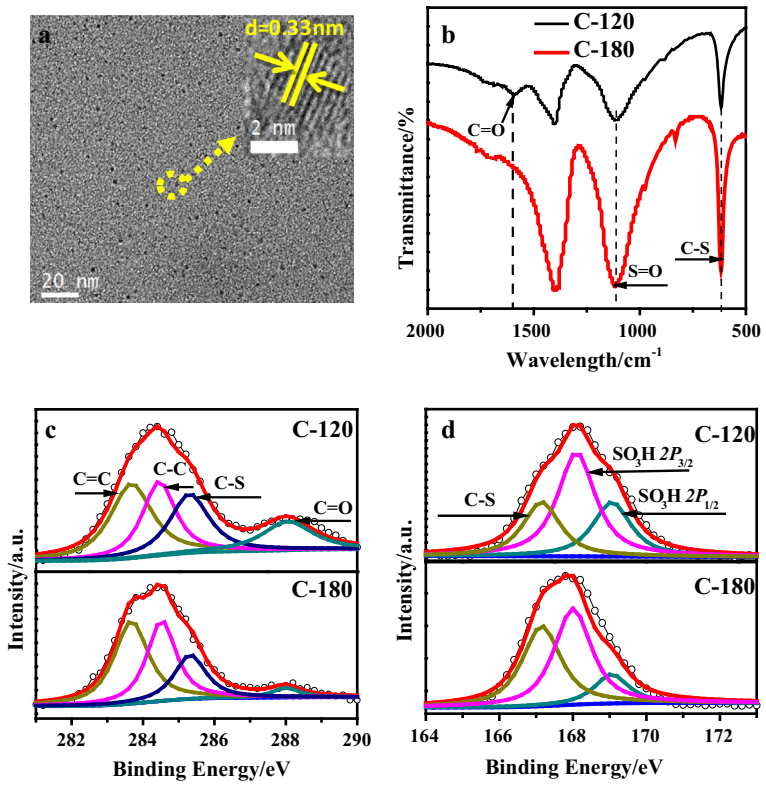

Fig. 1. (a) The TEM and HRTEM (inset) images of C-120. (b) FTIR spectra of C-120 and C-180. High-resolution XPS spectra of C-120 and C-180. (c) C1*s* and (d) S2*p* spectra.

284.5 eV), sp^2 bonded carbon (C═C, 283.6 eV), and carbonyl (C═O, 288.8 eV) [24,25]. For C-120, the ratio of —C═O to the total C bonds is 0.19 (Table S2), which is much higher than the 0.11 of C-180. Similar results could also be observed for H-120 (0.18) and H-180 (0.10). In S2*p* spectra (Fig. 1d), there are three contributions at 167.1, 168.0, and 169.1 eV, which are associated with sulfur in C-S, SO_3H $2P_{3/2}$, and SO_3H $2P_{1/2}$ groups [26], respectively. In addition, the change of sulfur content at different temperatures demonstrated that the SO_3H content gradually increased with increasing temperature (Table S1). Based on this method, it is easy to control the oxygen functional groups on the surfaces of CDs and provide a facile way to study their influences on electron transfer and photooxidation.

The major absorption band of CDs is located at 229 nm, which can be attributed to the $\pi \rightarrow \pi^*$ transition of the graphite structure. This result is consistent with the TEM images, XRD, and Raman spectra. Broadband absorption ranging from 350 to 600 nm could be attributed to the $n \rightarrow \pi^*$ transition of the C═O bonds [20]. Compared with the absorption of C-180, C-120 shows stronger absorption ability within this range (Fig. 2a), indicating that C-120 contains more C═O bonds than others. The stronger visible light absorption ability of C-120 would benefit the photocatalysis. The photoluminescence of C-120 is shown in Fig. 2b. The photoluminescence of the other CQDs is shown in Fig. S2. C-120 excited by 350 nm UV light shows strong yellow photoluminescence centered at 510 nm. Interestingly, even if petroleum coke with a complicated structure is used as a feedstock, the emission wavelength of C-120 is independent of the excitation wavelength ranging from 300 nm to 440 nm. This indicates that CDs derived from petroleum coke have a uniform distribution of functional groups on the surface of CDs, which benefits the following study of spectra [20,27,28].

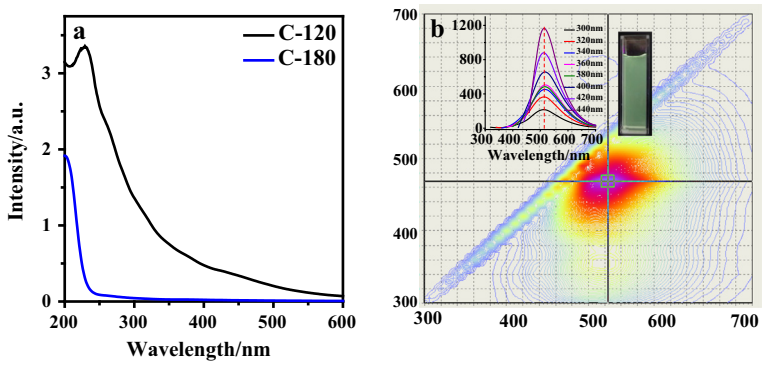

Fig. 2. (a) UV–vis absorption spectra of C-120 and C-180 (c = 0.15 mg•mL^{-1}, 20 °C in aqueous solution). (b) 3D luminescence plot of C-120 in aqueous solutions at room temperature and the emission spectra (inset) of C-120 excited by different excitation wavelengths from 300 nm to 440 nm (c = 0.15 mg•mL^{-1}, 20 °C in aqueous solution).

3.3. Application of carbon dots to photooxidation of 1,4-DHP

CDs are excellent candidates for photocatalysis due to their unique electron transfer ability. In order to investigate the influence of oxygen-containing functional groups of CDs on photooxidation, the photooxidation of 1,4-DHP was carried out by C-120 and C-180 (Fig. S4) in air. When the mixed solution of CDs and 1,4-DHP is irradiated with a xenon lamp, the absorption of 1,4-DHP at 374 nm decreases gradually, which can be demonstrated by the changes of UV curves and the rate of the reactions (k_{obs}). For C-120, the conversion rate of 1,4-DHP comes to 99.99% after irradiation for 30 min (Fig. 3b). For C-180, the conversion of 1,4-DHP is only 15.16% (Fig. 3b). The photooxidation velocities of CDs were studied by plotting the $\ln(A_t/A_0) - t$ curves (Fig. S4e). The slope (k_{obs}) of the photooxidation with C-120 is 0.13 min^{-1}, which is 22.8 times higher than that of C-180 (5.70×10^{-3} min^{-1}, Fig, S2e and Table S3). Furthermore, the photocatalytic stabilities of C-120 were investigated in the following repeated experiments. A concentrated solution of 1,4-DHP was added three times to the origin solution. As shown in Fig. 3c, 1,4-DHP is quickly photocatalyzed without any significant loss of photooxidation activity. The conversion of 1,4-DHP in repeat experiments is 98.97, 97.81, and 97.69%, respectively. In addition, the photostability of carbon dots and 1,4-DHP was also investigated by irradiating CDs and 1,4-DHP alone (Figs. S4d and S5). Obviously, little decrease of CDs' UV absorption was observed within 3 h. All CDs exhibit excellent photostability.

3.4. Mechanism of photooxidation

The electron transfer mechanism of this photooxidation was studied with ESR spectroscopy (Figs. 4a and S6). 5,5-Dimethyl-1-pyrroline-N-oxide (DMPO) [29] and 2,2,6,6-tetramethyl piperidine (TEMP) [30] were employed as scavengers for superoxide radical anion ($O_2^{-}\cdot$) and singlet state oxygen ($^1O_2$), respectively. With DMPO, the ESR signal of $O_2^{-}\cdot$ adduct was detected for the mixture of CDs and substrate 1,4-DHP upon photoirradiation (Fig. 4a). No such signal is detected in the absence of CDs or 1,4-DHP (Fig. S6a and b), indicating that electron transfer from 1,4-DHP to CDs is crucial for the formation of $O_2^{-}\cdot$. The experiment with TEMP shows that $^1O_2$ was produced with CDs in the absence of 1,4-DHP (Fig. S6c). With the addition of 1,4-DHP (Fig. S6d), no ESR signal of $^1O_2$ was detected, indicating that production of $^1O_2$ (generally, a low $^1O_2$ quantum yield indicates a poor energy transfer efficiency, which is competed with electron transfer) is completely inhibited by electron transfer from 1,4-DHP to CDs. Therefore, electron transfer between CDs and the substrate (1,4-DHP) is crucial for the photocatalysis process.

A mechanism involving electron transfer for the photooxidative aromatization of 1,4-DHP catalyzed by CDs is proposed in Fig. 4b. First, CDs are photoexcited into the excited state (CDs*). Electron transfer from 1,4-DHP (electron donor) to CDs* (electron acceptor) can produce highly active 1,4-DHP cation radicals, which are preferable to release H^+ subsequently. During this step, the enhanced electron-accepting ability of CDs could improve their photocatalytic ability. Then electron transfer from 1,4-DHP radicals to O_2 results in the production of final aromatization product 1b and reactive oxygen radicals ($O_2^{\cdot}$). $O_2^{\cdot}$ can grab electrons from CD radicals (electron donor), which could recover the photocatalyst and produce the superoxide anion radical ($O_2^{-}\cdot$). Last, H_2O_2 is generated by the reaction of $O_2^{-}\cdot$ and H^+. Due to the presence of CDs, H_2O_2 is decomposed into O_2 and H_2O [31], which meets the demands of green chemistry and produces no environmental pollution.

3.5. Effects of carbon dot surface structures on electron transfer

According to this mechanism of photooxidation, CDs play the roles of electron donor and acceptor. To confirm the relationship of functional groups of CDs and electron transfer, CDs with —C=O and/or —S=O are obtained by selecting different oxidation reagents, preparation temperatures, and reduction methods. For evaluation of —C=O in CDs, C-120 is obtained by the oxidation of HNO_3 and H_2SO_4 at 120 °C, and it contains both —C=O and —S=O. As the temperature increases to 180 °C, C-180 is obtained with fewer C=O groups, which has been confirmed by XPS and FT-IR in Fig. 1c and d. C-120 is reduced to R-120 by phenylhydrazine to

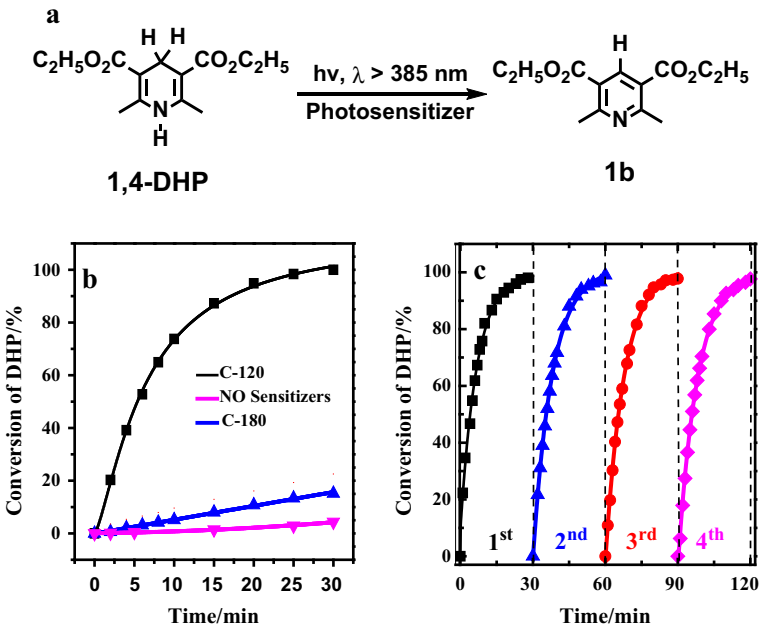

Fig. 3. (a) The photooxidation of 1,4-DHP by CDs as photosensitizers. (b) The yield of 1,4-DHP against irradiation time catalyzed by CDs. (c) Repetitive photooxidation of 1,4-DHP by C-120.

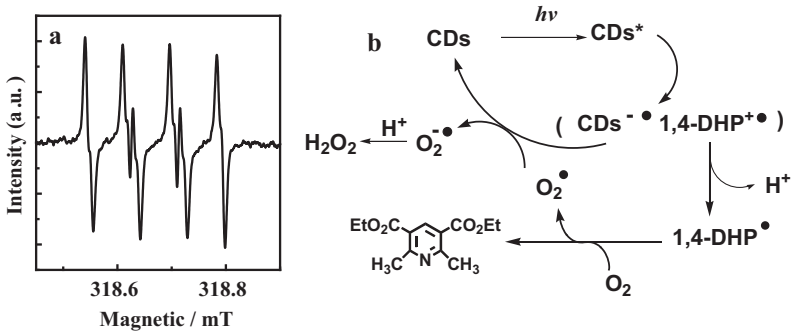

Fig. 4. (a) ESR spectrum upon photoirradiation of CDs (1.5 mg/mL), 1,4-DHP (1.0×10^{-4} M), and DMPO (1.0×10^{-2} M). (b) Mechanism for the photooxidation of 1,4-DHP with CDs as photosensitizer.

further investigate the influence of —C═O. The groups of R-120 demonstrated by XPS and FT-IR are given in Fig. S7. To investigating the effect of sole —S═O, H-120 and H-180 are prepared from oxidation with HNO_3 at 120 and 180 °C, in which there is no —S═O in CDs (Fig. S8).

Although CDs can hardly be regarded as a member of the semiconductor family, the quenching photoluminescence from CDs with either electron acceptor or electron donor molecules might also be a result of radiative recombination of surface-trapped electrons and holes [32]. To some extent, such quenching photoluminescence in CDs could quantitatively estimate the electron transfer, and the band structure (conduct band and valance band) examined by XPS and PL spectra could help to further understand the inherent impetus for the electron transfer.

3.5.1. Electron-accepting abilities of carbon dots

Triethanolamine (TEOA) was used as an electron donor to measure the electron-accepting ability of CDs [33]. Both —C═O and —S═O can enhance the electron-accepting properties of CDs. To confirm the performance of —C═O, C-120 (more —C═O and —S═O) is reduced to R-120 (—S═O and fewer —C═O groups). The Stern–Volmer quenching constant of C-120 *K*sv comes to 358 M^{-1} (Fig. 5a and Table S3), while the *K*sv of R-120 is only 9 M^{-1} (Fig. S9 and Table S3), resulting in a lower photooxidation yield of 1,4-DHP (14.25%, Fig. S10). To confirm the performance of —S═O in CDs, H-120 and H-180 without —S═O were prepared by HNO_3 oxidation. The K_{SV} of H-120 and H-180 (less —C═O groups in comparison with H-120) are only 102 and 6 M^{-1} (Fig. S9 and Table S3), and the photooxidation yields of 1,4-DHP are 81.31 and 8.08%, respectively (Fig. S11). The differences of H-120 and H-180 in *K*sv and photooxidation yield also demonstrate the influence of —C═O.

The influence of electron-withdrawing groups on the electron-accepting ability of CDs was elaborately studied by the valence bands (VBs) of CDs, which were further examined by XPS as shown in Fig. S12 and Table S4. Here, the VB position of C-120 (1.76 eV) is higher than others, which indicates that the accepting ability of C-120 is the highest among the studied samples. The results were consistent with their photooxidation performance.

3.5.2. Electron-donating properties of carbon dots

Different concentrations of *N,N*-methylviologen (MV) [34] were added to the solution of CDs to detect the electron-donating properties of CDs (Figs. 5b and S13). Interestingly, although C-120 contains more electron-withdrawing groups (e.g., —C═O and —S═O), the Stern–Volmer quenching constant (*K*sv) of C-120 comes to

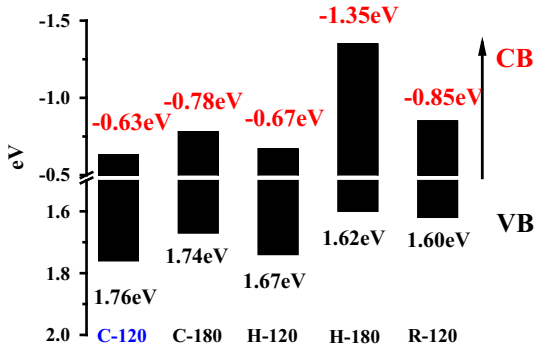

Fig. 6. The VB position, CB position, and band gap energy for C-120, C-180, H-120, H-180, and R-120.

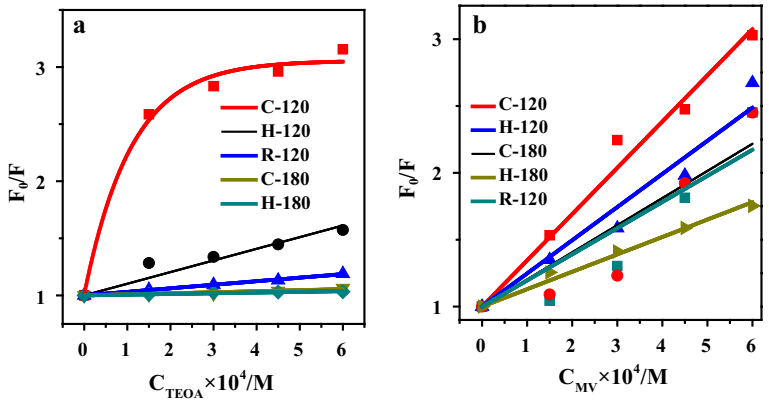

Fig. 5. (a) Stern–Volmer plot of the emission intensity of CDs with various amounts of TEOA upon excitation at 350 nm in H_2O. (b) Stern–Volmer plot of the emission intensity of CDs with various amounts of MV upon excitation at 350 nm in H_2O.

350 M^{-1}, which is higher than the 250 M^{-1} of H-120 (no —S═O), 200 M^{-1} of R-120 (less —C═O), 210 M^{-1} of C-180 (less C═O), and 130 M^{-1} of H-180 (less —C═O and no —S═O). This indicates that both —C═O and —S═O groups can promote the electron-donating ability of CDs.

The influence of electron-withdrawing groups on the electron-donating ability of CDs was elaborately studied by the conduction bands (CBs) of CDs, which were obtained by the VBs and the gap energy of CDs calculated from the maximum fluorescent emission (Fig. S2). The CB position of C-120 (−0.63 eV) is higher than others, which demonstrates that the electron-donating ability of C-120 is higher than others (see Fig. 6).

4. Conclusions

The surface electron-withdrawing groups (—C═O and —S═O) of CDs could enhance both electron-accepting and -donating abilities, thus effectively enhancing the photooxidation performance of 1,4-DHP. The introduced amounts of —C═O and —S═O groups can be facilely controlled via different oxidative and reducing agents and oxidation temperature. With the highest VB and CB, C-120 prepared from petroleum coke by HNO_3 and H_2SO_4 oxidation shows the highest electron transfer ability. As a result, the photocatalytic performance of C-120 (containing both —C═O and —S═O) is 6.6 times higher than that of C-180 (less —C═O) and 1.3 times higher than that of H-120 (no —S═O). This work may provide a feasible and effective strategy to solve the poor electron transfer ability of carbon dots and other carbon materials, which also helps in the value-added application of cheap and abundant carbon precursors.

Acknowledgments

This work was financially supported by the NSFC (21302224, 51172285, 51672309, 51372277, and 21406269), the China Postdoctoral Science Foundation (2014M560590 and 2015T80758), the Shandong Provincial Natural Science Foundation (ZR2013BQ028, ZR2013EMQ013, and ZR2014BQ012), the Shandong Provincial Key Research Program (Grant: 2015GSF121017), the Project of Science and Technology Program for Basic Research of Qingdao (14-2-4-47-jch), and the Fundamental Research Funds for Central Universities (15CX05010A, 15CX08005A, and 15CX05013A).

Appendix A. Supplementary material

Supplementary data associated with this article can be found, in the online version, at http://dx.doi.org/10.1016/j.jcat.2016.09.006.

References

[1] X. Xu, R. Ray, Y. Gu, H.J. Ploehn, L. Gearheart, K. Raker, W.A. Scrivens, J. Am. Chem. Soc. 126 (2004) 12736–12737.
[2] H. Li, Z. Kang, Y. Liu, S.T. Lee, J. Mater. Chem. 22 (2012) 24230–24253.
[3] W. Wu, L. Zhan, W. Fan, J. Song, X. Li, Z. Li, R. Wang, J. Zhang, J. Zheng, M. Wu, H. Zeng, Angew. Chem. Int. Ed. 127 (2015) 6640–6644.
[4] C. Ding, A. Zhu, Y. Tian, Acc. Chem. Res. 47 (2013) 20–30.
[5] Q. Liu, B. Guo, Z. Rao, B. Zhang, J.R. Gong, Nano. Lett. 13 (2013) 2436–2441.
[6] S. Chandraabc, P. Patrac, S.H. Pathand, S. Royc, S. Mitrac, A. Layeke, R. Bharb, P. Pramanik, A. Goswami, J. Mater. Chem. B 1 (2013) 2375–2382.
[7] X. Li, S. Zhang, S.A. Kulinich, Y. Liu, H. Zeng, Sci. Rep. 4 (2014) 4976–4983.
[8] H. Li, R. Liu, Y. Liu, H. Huang, H. Yu, H. Ming, S. Lian, S.T. Lee, Z. Kang, J. Mater. Chem. 22 (2012) 17470–17475.
[9] C. Hu, C. Yu, M. Li, X. Wang, Q. Dong, G. Wang, J. Qiu, Chem. Commun. 51 (2015) 3419–3422.
[10] M. Li, C. Hu, C. Yu, S. Wang, P. Zhang, J. Qiu, Carbon 91 (2015) 291–297.
[11] R. Ye, C. Xiang, J. Lin, Z. Peng, K. Huang, Z. Yan, N.P. Cook, E.L.G. Samuel, C.C. Hwang, G. Ruan, G. Ceriotti, A.O. Raji, A.A. Martí, J.M. Tour, Nat. Commun. 4 (2013) 2943–2948.
[12] C. Hu, C. Yu, M. Li, X. Wang, J. Yang, Z. Zhao, A. Eychmüller, Y.P. Sun, J. Qiu, Small 10 (2014) 4926–4933.
[13] M. Wu, Q. Zha, J. Qiu, X. Han, Y. Guo, Z. Li, A. Yuan, X. Sun, Fuel 84 (2005) 1992–1997.
[14] M. Wu, Y. Wang, W. Wu, C. Hu, X. Wang, J. Zheng, Z. Li, B. Jiang, J. Qiu, Carbon 78 (2014) 480–489.
[15] D.J. Martin, N. Umezawa, X. Chen, J. Ye, J. Tang, Energy Environ. Sci. 6 (2013) 3380–3386.
[16] K. Burkhard, Chemical Photocatalysis, Germany, 2013, pp. 185–199.
[17] K. Burkhard, Chemical Photocatalysis, Germany, 2013, pp. 211–217.
[18] J. Liu, Y. Liu, N. Liu, Y. Han, X. Zhang, H. Huang, Y. Lifshitz, S.T. Lee, J. Zhong, Z. Kang, Science 347 (2015) 970–974.
[19] W. Wu, J. Zhang, W. Fan, Z. Li, L. Wang, X. Li, Y. Wang, R. Wang, J. Zheng, M. Wu, H. Zeng, ACS Catal. 6 (2016) 3365–3371.
[20] M. Li, S.K. Cushing, X. Zhou, S. Guo, N. Wu, J. Mater. Chem. 22 (2012) 23374–23379.
[21] Z. Kang, E. Wang, B. Mao, Z. Su, L. Gao, S. Lian, L. Xu, J. Am. Chem. Soc. 127 (2005) 6534–6535.
[22] M. Zhang, L. Bai, W. Shang, W. Xie, H. Ma, Y. Fu, D. Fang, H. Sun, L. Fan, M. Han, C. Liu, S. Yang, J. Mater. Chem. 22 (2012) 7461–7467.
[23] Y. Dong, H. Pang, H. Yang, C. Guo, J. Shao, Y. Chi, C.M. Li, T. Yu, Angew. Chem. Int. Ed. 52 (2013) 7800–7804.
[24] J. Lu, J.X. Yang, J. Wang, A. Lim, S. Wang, K.P. Loh, ACS Nano 3 (2009) 2367–2375.
[25] A.K. Flatt, B. Chen, J.M. Tour, J. Am. Chem. Soc. 127 (2005) 8918–8919.
[26] S.L. Hu, K.Y. Niu, J. Sun, J. Yang, N.Q. Zhao, X.W. Du, J. Mater. Chem. 19 (2009) 484–488.
[27] Q.L. Zhao, Z.L. Zhang, B.H. Huang, J. Peng, M. Zhang, D.W. Pang, Chem. Commun. 41 (2008) 5116–5118.
[28] Y. Wang, L. Dong, R. Xiong, A. Hu, J. Mater. Chem. C1 (2013) 7731–7735.
[29] J.J. Huang, Z.F. Zhong, M.Z. Rong, X. Zhou, X.D. Chen, M.Q. Zhang, Carbon 70 (2014) 190–198.
[30] A. Kładna, P. Berczyński, T. Piechowska, I. Kruk, H.Y.A. Enein, M.C. Unlusoy, E.J. Verspohl, R. Ertan, Luminescence 29 (2014) 846–853.
[31] K. Ergaieg, M. Chevanne, J. Cillard, R. Seux, Sol. Energy 82 (2008) 1107–1117.
[32] F. Chen, X. Zhao, H. Liu, J. Qu, Chem. Eng. J. 253 (2014) 478–485.
[33] X. Wang, L. Cao, F. Lu, M.J. Meziani, H. Li, G. Qi, B. Zhou, B.A. Harruff, F. Kermarrec, Y.P. Sun, Chem. Commun. 25 (2009) 3774–3776.
[34] V. Strauss, J.T. Margraf, C. Dolle, B. Butz, T.J. Nacken, J. Walter, W. Bauer, W. Peukert, E. Spiecker, T. Clark, D.M. Guldi, J. Am. Chem. Soc. 136 (2014) 17308–17316.